FINITE ELEMENT METHOD ON EARTHQUAKE FAULT RUPTURE PROPAGATION THROUGH COHESIONLESS SOIL WITH SPATIAL VARIABILITY

Lipon Paul*[1], Md. Rokonuzzaman[2], Nibir Rahman[3] and A.Wadud Ruhani[4]

[1]Post Graduate Student, Department of Civil Engineering, KUET Khulna, Bangladesh, e-mail:liponcekuet@gmail.com
[2] Professor, Khulna University of Engineering & Technology (KUET), Khulna, Bangladesh, e-mail: rokon@ce.kuet.ac.bd
[3] Lecturer, Khulna University of Engineering & Technology (KUET), Khulna, Bangladesh, e-mail: nibir@ce.kuet.ac.bd
[4] Graduate, Department of Civil Engineering, KUET Khulna, Bangladesh, e-mail: ruhani1901065@stud.kuet.ac.bd

***Corresponding Author**

ABSTRACT

Earthquake fault rupture propagation may cause significant differential settlement in the ground surface. When fault ruptures occur in or adjacent to the existing structures, considerable damage can result. In most geotechnical designs, the soil is considered homogeneous and isotropic, but soil is generally heterogeneous and anisotropic in nature. So that the differential settlement is underestimated in most of the designs. In this paper, a finite element method is used to find the zone of differential settlement in the ground surface in cohesionless soil due to earthquake fault rupture propagation with normal fault rupture and dip angle of 60^o. The influence of soil variability was quantified through the coefficient of variation (COV) and correlation length (CL) using a Monte Carlo Simulation. Results demonstrate that increasing COV widens the deformation zone and reduces surface rupture angle, reflecting the role of weak pockets in diffusing rupture energy. Similarly, longer correlation lengths promote broader, smoother deformation profiles, while shorter lengths confine rupture to narrow, localized bands. This study highlights the necessity of incorporating spatial variability into fault rupture hazard assessment, considering the soil as heterogeneous and isotropic. The findings provide new insights into rupture mechanics and offer a framework for risk-informed design and land use planning in seismically active regions.

Keywords: *Fault rupture, coefficient of variation (COV), correlation length (CL), homogeneous, heterogeneous, isotropic.*

1. INTRODUCTION

In recent years, earthquakes have become a more concerning issue all over the world. Fault rupture in a tectonic plate propagating through cohesionless soil can cause significant damage to the ground surface. The geotechnical engineers need to understand the fault rupture propagation through the overlaying sand mass at the site and design a structure near or across the fault plane. Incorporating soil heterogeneity into fault rupture analysis is not merely a refinement—it is a necessity for accurate hazard assessment and resilient design. By considering heterogeneity, engineers can identify zones of elevated risk, design foundations that accommodate differential movement, and establish setback distances that reflect actual rupture potential. Experimental studies and numerical simulations have shown that heterogeneity can cause rupture to emerge at unexpected locations, sometimes far from the vertical projection of the fault plane. These deviations are critical for delineating hazard zones and designing safe setback distances. Traditional deterministic models assume uniform soil properties and fixed fault geometries, leading to singular predictions of rupture path and surface deformation. While useful for preliminary analysis, these models fail to capture the variability observed in field cases and experiments. Deterministic approaches cannot account for uncertainty in soil parameters, nor can they estimate the probability of rupture emergence at different locations. As a result, they may underestimate the extent of deformation zones or misidentify safe construction areas. In seismic design and hazard assessment, relying solely on deterministic models can lead to non-conservative decisions and increased vulnerability. A key component of probabilistic modeling is the generation of spatially variable soil properties using random fields. This involves defining a mean value, coefficient of variation (COV), and correlation length for each parameter of interest, such as friction angle or stiffness. The COV quantifies the relative variability of the property, while the correlation length determines the spatial scale over which values are correlated. For example, a high COV with a short correlation length produces a highly variable field with frequent changes, whereas a low COV with a long correlation length yields smoother transitions. These parameters are derived from site investigations, laboratory tests, and empirical studies. Incorporating soil heterogeneity into fault rupture analysis is not merely a refinement—it is a necessity for accurate hazard assessment and resilient design. Field evidence from earthquakes such as Chi-Chi in Taiwan (Bray, 2001), Kocaeli in Turkey (Pamuk et al., 2005), and Hebgen Lake (Witkind et al., 1962) consistently shows that local soil conditions influence rupture behavior. Structures built on seemingly stable ground have failed due to unexpected rupture emergence, while others have survived due to fortuitous diversion (Bray, 2001). Homogeneous models cannot explain these outcomes and require probabilistic frameworks that account for variability.

Early sandbox experiments (Sanford, 1959) showed that dip-slip dislocations in sand produce shear bands that refract toward the surface. Cole & Lade (1984) systematically studied rupture in dense and loose sands, identifying the role of density in controlling rupture localization. By the late 20th century, centrifuge modeling emerged as a powerful tool. Roth, Scott, et al., (1981) conducted some of the earliest centrifuge tests, showing how rupture paths refract and sometimes die out in loose alluvial soils. Later, Anastasopoulos et al., (2007) validated finite element predictions against centrifuge data, achieving “Class A” predictions of rupture location and surface deformation. Parallel advances in numerical modeling (Scott & Schoustra, 1974; Bray et al., 1994; Loukidis et al., 2009) introduced elastoplastic constitutive laws with strain softening, enabling realistic simulation of shear band formation. These studies bridged the gap between descriptive geology and predictive geotechnical modeling. Loose sands: deformation spreads over a wide zone; rupture may dissipate before reaching the surface. Dense sands: deformation localizes; rupture is more likely to outcrop as a distinct scarp. This density dependence was confirmed in centrifuge tests (Anastasopoulos et al., 2007; Rokonuzzaman et al., 2015) and numerical studies (Loukidis et al., 2009). Random field theory provides a framework to model spatial variability by treating soil properties as stochastic fields with defined mean, variance, and correlation length. This approach has been successfully applied to:(1) Slope stability (Griffiths & Fenton, 1993) (2) Bearing capacity (Fenton & Griffiths, 2003) (3) Liquefaction triggering (Popescu et al., 2006). To date, few studies have applied random field theory to fault rupture. Most existing models (Seed, 1982; Anastasopoulos et al., 2007; Loukidis et al., 2009; Rokonuzzaman et al., 2015) assume

homogeneous soils. However, in reality: Loose pockets may absorb rupture energy, dense zones may localize rupture and layering & variability may cause rupture bifurcation or arrest.

2. MODEL SETUP

The problem under consideration is inspired by the study of (Rokonuzzaman et al., 2015). The model dimensions and material parameters are followed by (Rokonuzzaman et al., 2015). Following the recommendation of (Bray et al., 1994), the length L of the finite element model was equal to 4H in order to minimize undesired boundary effects. Where L is the length of the finite element model 75.9 m. H is 24.6 m height of finite element model. W length of the hanging wall, equal to 24.15m. d represents the horizontal distance from the vertical projection of the fault trace in the bedrock and Δy represent the vertical displacement.

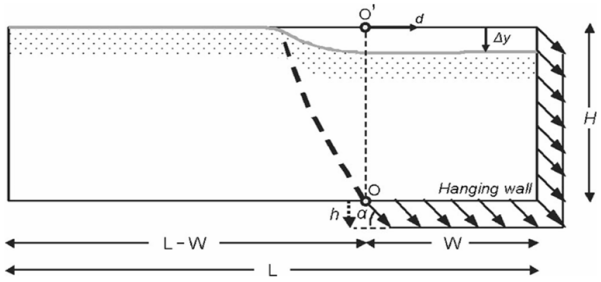

Figure 1: Basic model dimensions and definitions for normal faulting (Anastasopoulos et al., 2007)

The setup is as sketched in Figure 1. In the normal faulting configuration, the right and bottom walls are gradually moved downwards at a given inclination until a failure occurs. The left walls are immovable, while displacements are prescribed on the right walls. In OPTUM G2, displacement boundary conditions can be imposed with respect to structural elements only.

3. MODEL VALIDATION

Figure 2 represents a comparative analysis of fault rupture propagation through homogeneous cohesionless soil, based on elastoplastic simulations conducted in OPTUM G2 and experimental results from beam centrifuge tests by (Rokonuzzaman et al., 2015). In Figure 3, three vertical base dislocation values (h) 1.008 m, 1.558 m, and 2.046 m were considered to evaluate the surface deformation response. For each dislocation scenario, the vertical surface displacement profiles from the numerical model closely match the experimental curves, particularly in regions exhibiting steep displacement gradients. Although small differences in vertical displacement magnitudes are observed at specific horizontal distances but the rupture paths converge beyond these points. This consistency in rupture geometry confirms that the present elastoplastic analysis in OPTUM G2 reliably reproduces the fault propagation behavior observed in physical experiments.

(a)

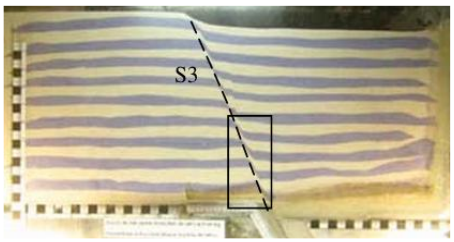

(b)

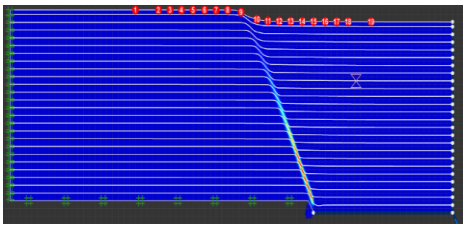

Figure 2: Comparison of rupture propagation path (a) centrifuge experiment (Rokonuzzaman et al., 2015) (b) FE model (present study) for h=2.046 m.

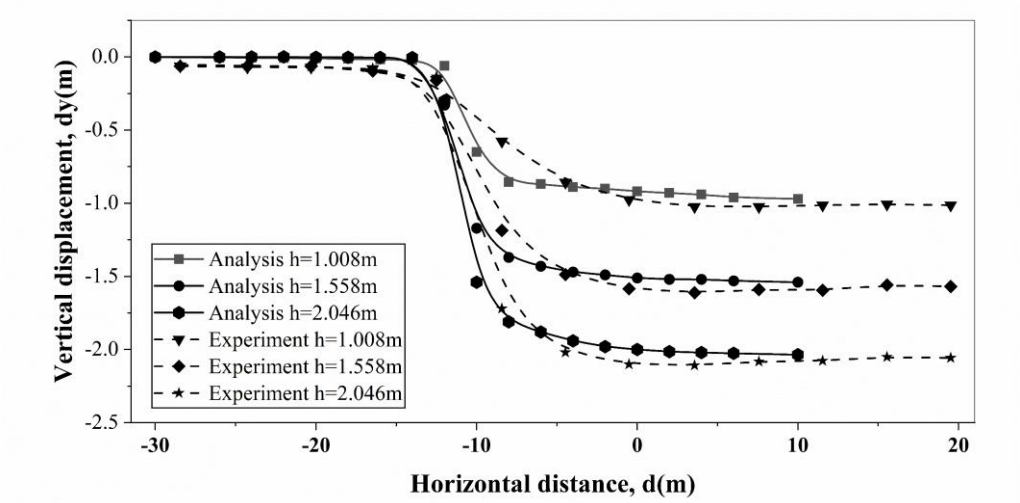

Figure 3: Comparison of vertical surface displacement in homogeneous soil with existing experimental results (Rokonuzzaman et al., 2015).

Table 1: Parameters of Mohr-Coulomb Sand used in the numerical simulation, followed by (Rokonuzzaman et al., 2015).

Dry unit weight, γ_{dry} (kN/m³)	15.57
Poisson's ratio, ν (-)	0.3
Cohesion, c (kPa)	0
Peak friction angle, ϕ (º)	35
Dilation angle, ψ (º)	6
Tensile strength, k_t (kPa)	0
Inclination of the tension cut-off cone, ϕ_t (º)	90
Young modulus, E (MPa)	$27.70\sqrt{z}$
Pressure coefficient at rest, K_0	0.5

Where, z = vertical distance from the ground surface.

4. STOCHASTIC ANALYSIS

Natural soils display a considerable amount of variability, the origins of which can be traced to a variety of processes at a range of length scales. This variability can be taken into account in a number of ways. The simplest is to assume that a given parameter of interest, the friction angle for example, follows a probability distribution given by a mean value and standard deviation. The variability of such parameters is often modeled using the lognormal distribution. The log-normal distribution of $\sigma_{ø}$, $\mu_{ø}$ is computed by

$$\sigma_{ln\,ø} = \sqrt{ln\left[1 + \left(\frac{\sigma_ø}{\mu_ø}\right)^2\right]} \quad (1)$$

$$\mu_{ln\,ø} = ln\,\mu_ø - \frac{1}{2}(\sigma_{ln\,ø})^2 \quad (2)$$

The model uses a log-normal function for the probability distribution, given by

$$f(x;\mu,\sigma) = \frac{1}{x\sigma\sqrt{2\pi}} exp\left[\frac{-(ln\,x-\mu)^2}{2\sigma^2}\right], x > 0 \quad (3)$$

Where f denotes the probability distribution function for the parameter x, and σ and μ indicate the standard deviation and mean, respectively.

5. PARAMETRIC STUDY

To assess the influence of geotechnical uncertainty on fault rupture propagation, four levels of coefficient of variation (COV) were adopted: 10%, 20%, 30% and 50%. These values span the typical range reported in the literature (Phoon & Kulhawy, 1999) and allow for evaluation of both moderate and extreme variability scenarios in the probabilistic framework, and the horizontal correlation length (CLx) for friction angle varies from 5-50m and the vertical correlation length (CLy) for friction angle varies from 0.5-2 m (Phoon, 1995).

Table 2**:** Range of spatial variability parameter

Reference	COV (friction angle) %	CLx (m)	CLy (m)
Isotropic	10,20,30,50	0.5,1.0,2.0	0.5,1.0,2.0

5.1 Monte Carlo Simulation (MCS) and Random Field Generation

To know the effect of number of MCS first some result points are selected from figure 4 which are located at the steep slope of fault rupture propagation then the model had runed for 1,5,10,20,30,50,100,200,400,600 MCS and have taken the average vertical displacement for every point against different number of MCS and graph have drawn from the graph it has seen that after 200 MCS the vertical displacement for these points are not changed as shown in figure 5. This reason 200 MCS is selected to run the model in order to reduce the computational time.

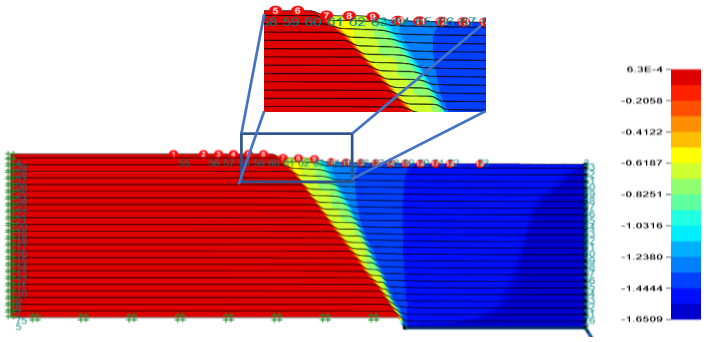

Figure 4: Vertical displacement of ground surface

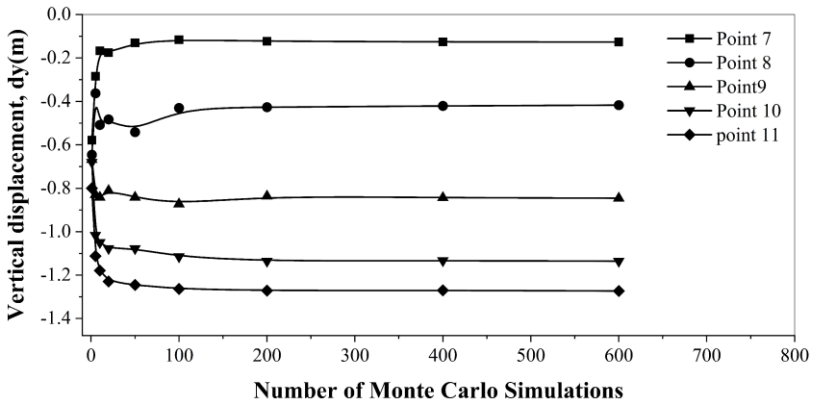

Figure 5: Effect of Number of Monte Carlo Simulations

5.2 Random Field Generation

The random field concept provides a means of generating more realistic spatial distributions of the material parameters. A probability distribution is still assumed to account for the inherent variability. In addition, vertical and horizontal correlation lengths are introduced, the idea being that a value of a material parameter measured at one point will have some correlation to the value measured at an adjacent point, depending on how far apart the two points are (vertically and horizontally). The correlation length describes the distance over which the measured values will tend to be significantly correlated. A large correlation length will thus imply a smoothly varying field, while a smaller value will imply a more ragged field.

A random ∅ (friction angle) field is generated using the technique of Karhunen-Loeve expansion (KL).

To generate a random field of a given material parameter, four input parameters are required:

1. The mean value of the parameter.
2. The coefficient of variation of the parameter, COV (%).
3. The horizontal correlation length of the parameter, CLx (m).
4. The vertical correlation length, CLy (m).

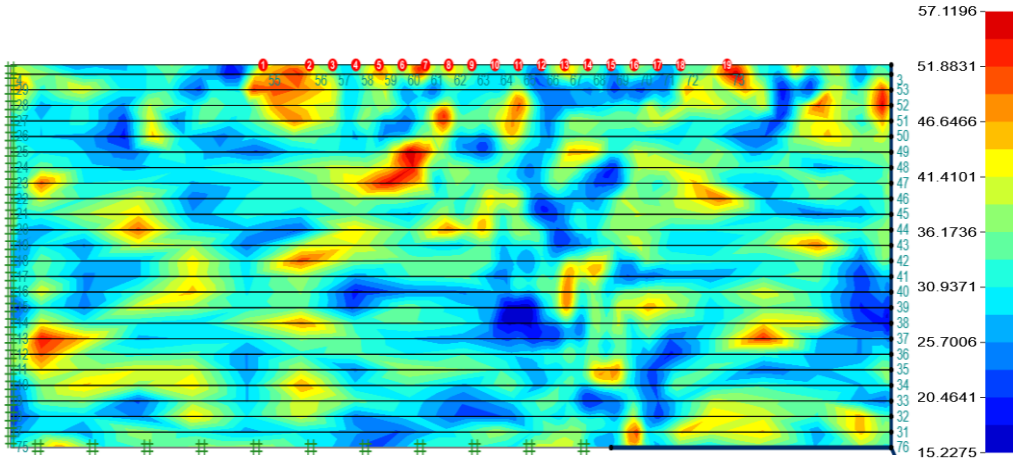

Figure 6: Random field generation for 20% COV, CLx=CLy=1.0m

5.3 Probability Distribution of Vertical Displacement on the Ground Surface.

To know the vertical displacement profile of the ground surface is one of the major objectives in this study.For this reason 19 result points has taken on the ground surface which is shown in figure 4. For 200 monte carlo simulation every result point gives 200 data of vertical displacement. Figure 7 shows the probability distribution of vertical displacement for result point 5 which is shown in figure 4. Here the mean vertical displacement has taken which is 0.01405 m downward. Following the same process for every result point mean vertical displacement has taken and vertical displacement profile of ground surface is drawn with respect to the horizontal distance.

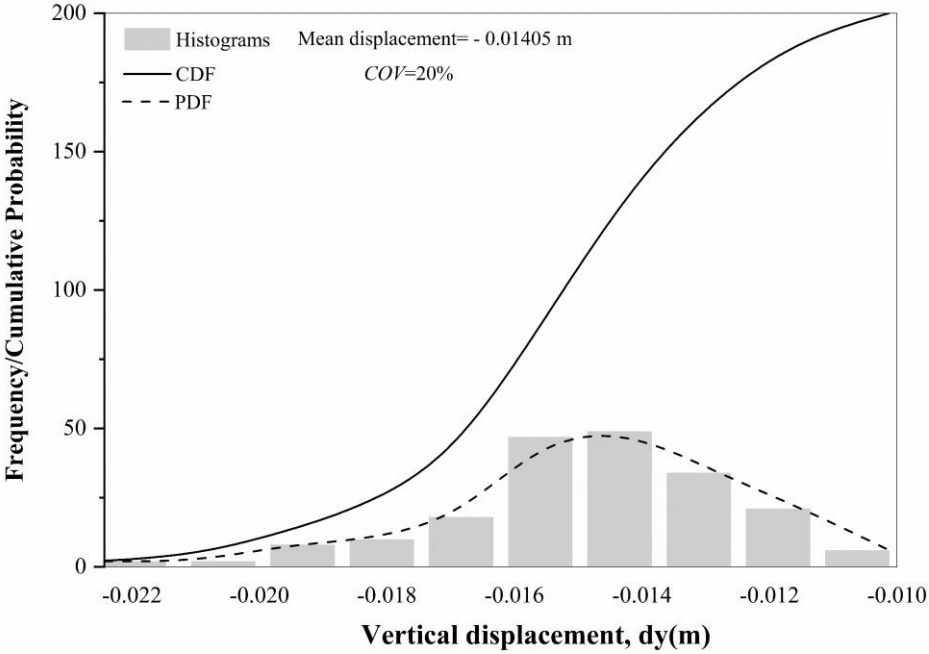

Figure 7: Probability distribution of vertical displacement, dy(m)

6. RESULT AND DISCUSSION

Result and discussion in this section compare the fault rupture propagation through

- Homogeneous and heterogeneous soil
- Isotropic soil (with different coefficients of variability and correlation length)

6.1 Fault rupture propagation through homogeneous and heterogeneous cohesionless soil

In Figure 8(a) the soil is homogeneous, characterized by a uniform friction angle of 35° and a coefficient of variation (COV) of 0%. The rupture path is distinctly defined, exhibiting a single, continuous shear band extending from the underlying fault to the ground surface. The surface deformation zone is narrow and well-localized, indicating strong strain concentration and minimal lateral dispersion. In contrast, Figure 8(b) illustrates rupture propagation in a heterogeneous soil mass with the same mean friction angle (35°) but a COV of 20%. In this case, the rupture path becomes more irregular and fragmented, forming multiple secondary branches rather than a single continuous trace. The deformation zone is considerably wider, displaying distributed strain localization and deviation of rupture paths into weaker zones within the soil. Such behavior reflects the natural variability of real soils, where heterogeneity promotes distributed faulting and broadens the surface rupture corridor. Consequently, hazard zones in heterogeneous deposits become more extensive and less predictable compared to the idealized homogeneous condition.

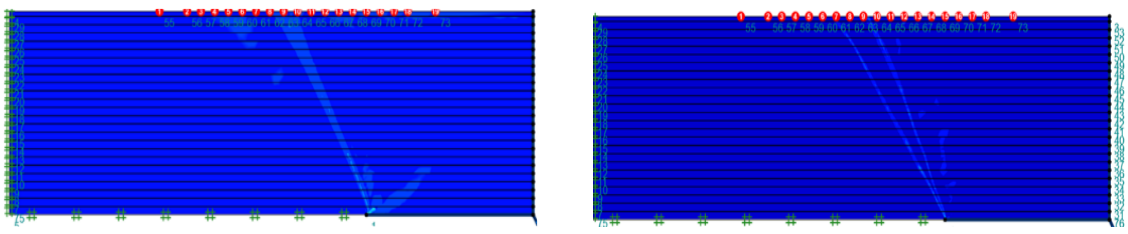

(a) Homogeneous soil (b) Heterogeneous soil

Figure 8: Fault rupture propagation through (a) homogeneous soil (b) heterogeneous soil

6.2 Comparison of Vertical Displacement of Ground Surface (Variation of COV Constant, Constant Correlation Length)

Figure 9 shows the comparison of vertical displacement profile of ground surface with variation of coefficient of variation (COV) for constant correlation length. For less coefficient of variability the vertical displacement profile of ground surface is more steeper. For 10% COV less weak zone creates and and rupture propagate without creating secondary rupture path this reason vertical displacement profile of ground surface is steep.For coefficient of variation greater than 20% more weak pockets creates and secondary rupture path developed which form garben in surface and vertical displacement profile of ground surface become wider.

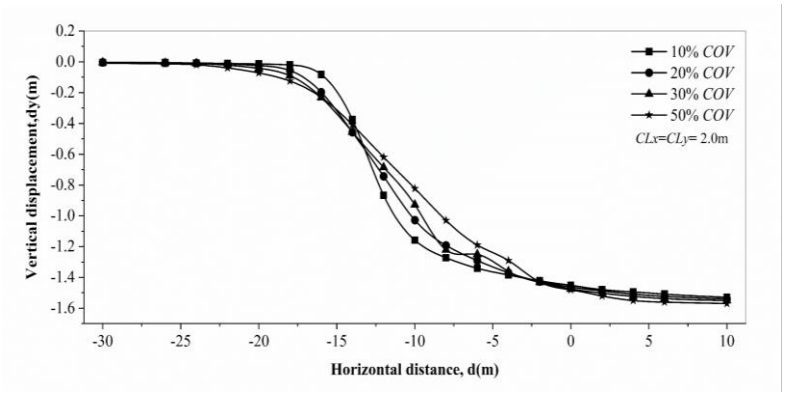

(a)

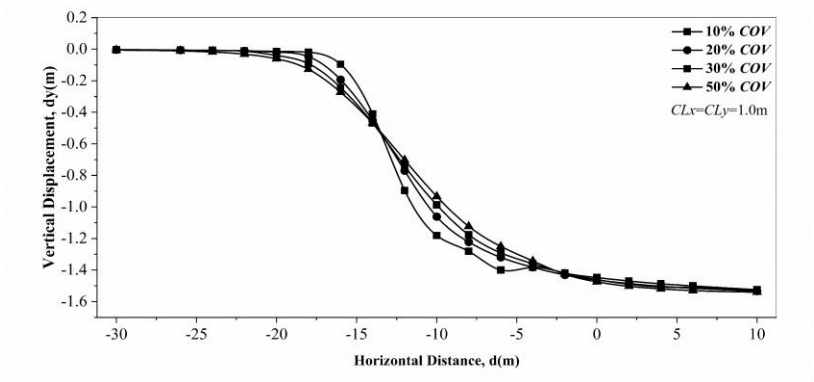

(b)

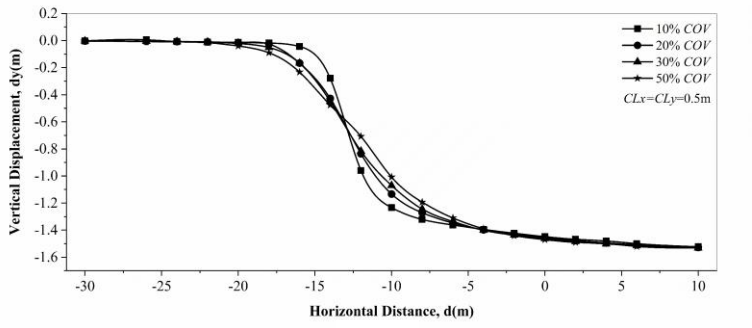

(c)

Figure 9: Comparison of vertical displacement of ground surface for variation of coefficient of variation (COV) with constant correlation length (a) 2 m, (b) 1 m, (c) 0.5 m.

6.3 Comparison of vertical displacement of ground surface (variation of correlation length with constant COV)

Figure 10 shows comparison of vertical displacement profile of ground surface for variation of correlation length with constant coefficient of variation for constant coefficient of variability with increasing correlation length the zone of weak pocket (where the value of friction angle is small) increasing and attract the rupture path to propagates for this reason with increasing correlation length secondary and tertiary rupture path form and propagates which affects the surface displacement profile and with increasing correlation length the vertical surface deformation profile become widen and flatten.

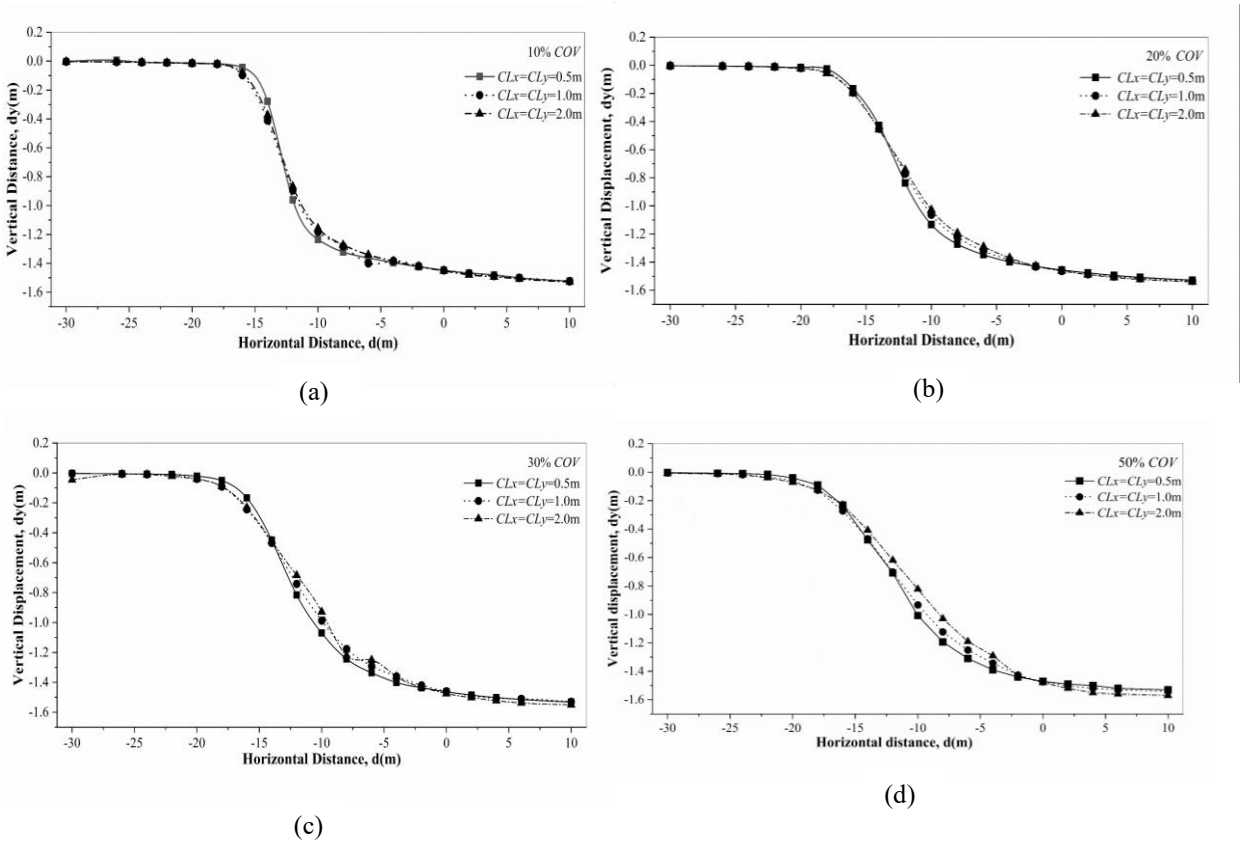

Figure 10: Comparison of vertical displacement of ground surface for variation of CL with constant COV (a) 10% COV (b) 20% COV (c) 30% COV (d) 50% COV.

6.4 Comparison of Ground Surface Inclination($\frac{dy}{dx}$) With Variation of Correlation Length For Constant COV

Ground surface inclination is important to find out the width of the deformation zone based on 0.2% (1\500) criterion as well as fault trace location on the ground surface (point of maximum ground surface inclination). Figure 11 shows that with increasing coefficient of variability the maximum ground surface inclination decreases. For correlation length 0.5m the maximum ground surface inclination for COV 10% is 0.26, for COV 20% this is 0.19 for COV 30% this is 0.17 and for COV 50% is 0.15, which indicates that with increasing COV, the maximum ground surface inclination decreases. For the same coefficient of variation, with increasing correlation length the ground surface inclination decreases. And for COV 30% and COV 50% with increasing correlation length, the peak surface inclination point moves right and the range lies between -10m and -15m.

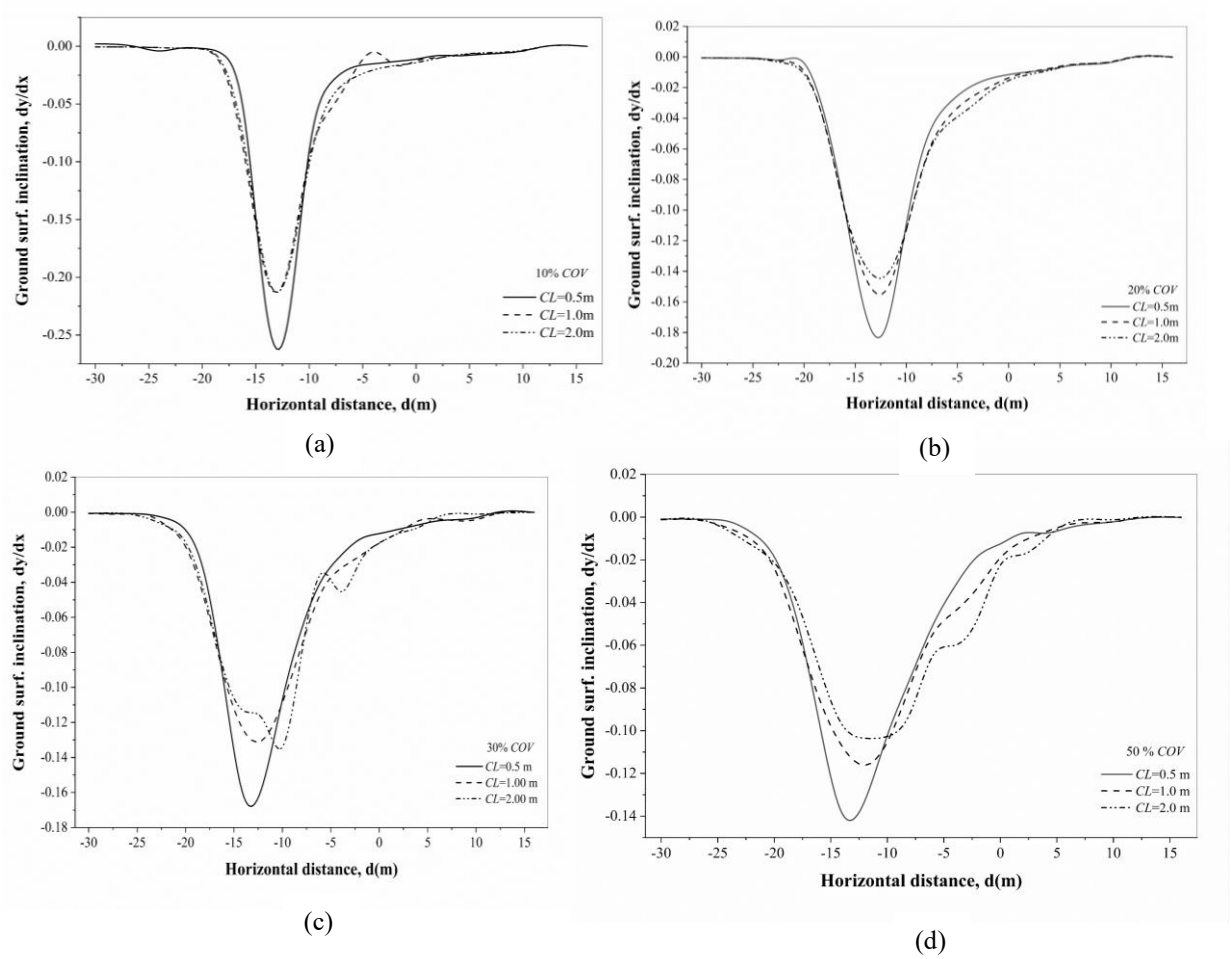

Figure 11: Comparison of ground surface inclination with variation of correlation length for constant COV (a) 10% COV (b) 20% COV (c) 30%COV (d) 50% COV

6.5 Comparison of Surface Displacement Profile Between Homogeneous and Heterogeneous Soil

Figure 12 (a) shows the variation of vertical surface displacement (dy) with horizontal distance (d) for two soil types: homogeneous isotropic, heterogeneous isotropic. The homogeneous isotropic soil exhibits a sharp, localized drop with limited deformation spread. In contrast, the heterogeneous isotropic soil displays a smoother and broader displacement curve, indicating that spatial variations in soil properties cause deformation to distribute over a wider region. Figure 12(b) shows the surface inclination with respect to horizontal distance, which is important to know the fault trace location on the ground surface and a significant ground distortion zone based on 0.2% criterion. For the same COV, the width of the deformation zone is less in homogeneous soil than in heterogeneous soil.

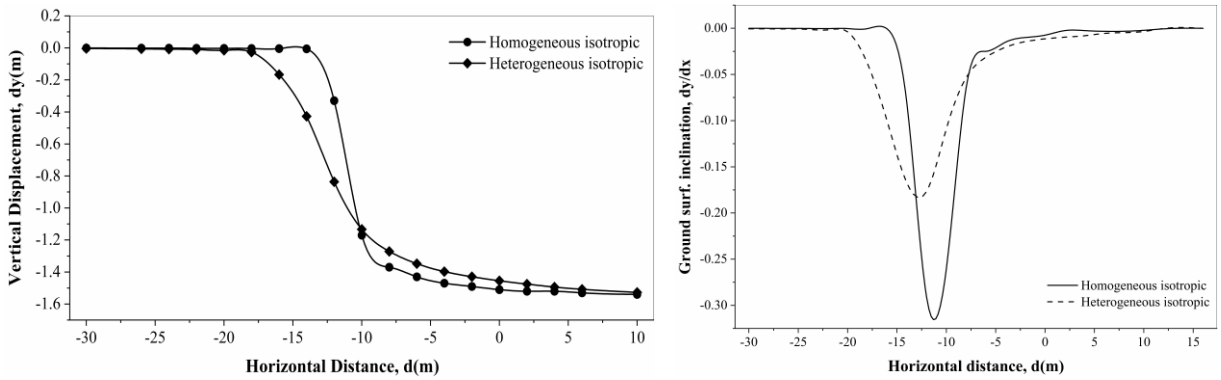

(a) (b)

Figure 12: Comparison between homogeneous isotropic and heterogeneous isotropic soil (a) surface displacement profile, (b) surface inclination.

7. CONCLUSIONS

This study investigates the effect of spatial variability on fault rupture propagation through cohesionless soils. Using finite element modeling integrated with random field theory, the study systematically examined the effects of homogeneous isotropic versus heterogeneous isotropic soils and the influence of coefficient of variation (COV) and correlation length (CL) on rupture geometry and deformation width.

The key conclusions are:

1. Homogeneous vs. Heterogeneous Soils: Homogeneous soils produced narrow, well-defined shear bands with strong localization. Heterogeneous soils (COV ≥ 20%) generated irregular rupture paths, branching, and wider deformation zones, reflecting the influence of weak pockets.

2. Effect of COV: Increasing COV consistently widened the deformation zone and reduced surface rupture angle. At high COV (30%), rupture became highly diffuse, with multiple strands and significant uncertainty in rupture location.

3. Effect of Correlation Length: Longer CL values promoted broader, smoother deformation zones and shallower rupture angles, as variability was spatially coherent. Short CL values produced patchy, localized rupture with steeper angles.

4. Surface Deformation Profiles: Both COV and CL controlled the width and angle of surface rupture. High COV with long CL produced the widest, flattest deformation zones, while low COV with short CL produced narrow, steep scarps.

Overall, the study demonstrates that spatial variability is a critical control on rupture propagation. Deterministic models that assume homogeneity underestimate the width and uncertainty of deformation zones. A probabilistic framework is therefore essential for realistic hazard assessment and risk-informed design.

ACKNOWLEDGEMENTS

The authors are grateful to the Khulna University of Engineering & Technology for providing the academic license of OPTUM G2.

REFERENCES:

Anastasopoulos, I., Gazetas, G., Bransby, M. F., Davies, M. C. R., & El Nahas, A. (2007). Fault Rupture Propagation through Sand: Finite-Element Analysis and Validation through Centrifuge Experiments. *Journal of Geotechnical and Geoenvironmental Engineering*, *133*(8), 943–958. https://doi.org/10.1061/(asce)1090-0241(2007)133:8(943)

Bray, J. D. (2001). Developing mitigation measures for the hazards associated with earthquake surface fault rupture. *A Workshop on Seismic Fault-Induced Failures – Possible Remedies for Damage to Urban Facilities*, *12355020*, 55–80. http://www.aegsc.org/meetings/Bray 2001- EQ Faulting.pdf

Bray, J. D., Seed, R. B., Cluff, L. S., & Seed, H. B. (1994). Earthquake Fault Rupture Propagation through Soil. *Journal of Geotechnical Engineering*, *120*(3), 543–561. https://doi.org/10.1061/(ASCE)0733-9410(1994)120:3(543)

Cole, D. A., & Lade, P. V. (1984). Influence zones in alluvium over dip-slip faults. *Journal of Geotechnical Engineering*, *110*(5), 599–615. https://doi.org/10.1061/(ASCE)0733-9410(1984)110:5(599)

Fenton, G. A., & Griffiths, D. V. (2003). Bearing-capacity prediction of spatially random c - ø soils. *Canadian Geotechnical Journal*, *40*(1), 54–65. https://doi.org/10.1139/t02-086

Griffiths, D. V., & Fenton, G. A. (1993). Seepage beneath water retaining structures founded on spatially random soil. *Geotechnique*, *43*(4), 577–587. https://doi.org/10.1680/geot.1993.43.4.577

Loukidis, D., Bouckovalas, G. D., & Papadimitriou, A. G. (2009). Analysis of fault rupture propagation through uniform soil cover. *Soil Dynamics and Earthquake Engineering*, *29*(11–12), 1389–1404. https://doi.org/10.1016/j.soildyn.2009.04.003

Pamuk, A., Kalkan, E., & Ling, H. I. (2005). Structural and geotechnical impacts of surface rupture on highway structures during recent earthquakes in Turkey. *Soil Dynamics and Earthquake Engineering*, *25*(7–10), 581–589. https://doi.org/10.1016/j.soildyn.2004.11.011

Phoon, K. K. (1995). Reliability-based design of foundations for transmission line structures. *Cornell University.*, *130*(2), 556. http://dx.doi.org/10.1016/j.jaci.2012.05.050

Phoon, K. K., & Kulhawy, F. H. (1999). Characterization of geotechnical variability. *Canadian Geotechnical Journal*, *36*(4), 612–624. https://doi.org/10.1139/t99-038

Popescu, R., Prevost, J. H., & Deodatis, G. (2006). 3D effects in seismic liquefaction of stochastically variable soil deposits. *Risk and Variability in Geotechnical Engineering: The Institution of Civil Engineers*, *1*, 81–91. https://doi.org/10.1680/ravige.34860.0008

Rokonuzzaman, M., Nahas, A. E., & Sakai, T. (2015). Experimental validation of a numerical model for the interaction of dip-slip normal fault ruptures, sand deposits, and raft foundations. *International Journal of Geotechnical Engineering*, *9*(3), 239–250. https://doi.org/10.1179/1939787914Y.0000000057

Roth, W. H., Scott, R. F., & Austin, I. (1981). Centrifuge modeling of fault propagation through alluvial soils. *Geophysical Research Letters*, *8*(6), 561–564.

Sanford, B. . Y. A. R. (1959). *Simple Geologic Structures*. *70*(January), 19–52.

Scott, R. F., & Schoustra, J. J. (1974). Nuclear Power Plant Siting on Deep Alluvium. *Journal of the Geotechnical Engineering Division*, *100*(4), 449–459. https://doi.org/10.1061/AJGEB6.0000037

Seed, H. B. (1982). Ground motions and soil liquefaction during earthquakes. *Earthquake Engineering Research Insititue*.

Witkind, I. J., Myers, W. B., Hadley, J. B., Hamilton, W., & Fraser, G. D. (1962). Geologic features of the earthquake at Hebgen Lake, Montana, August 17, 1959. *Bulletin of the Seismological Society of America*, *52*(2), 163–180.